Alternative female and male developmental strategies in the dynamic balance of human visual perception

Gergő Ziman[1,2,3], Stepan Aleshin[4], Zsolt Unoka[5], Jochen Braun[6], and Ilona Kovács[1,2,7]

[1]Laboratory for Psychological Research, Pázmány Péter Catholic University, Budapest, Hungary
[2]Adolescent Development Research Group, Hungarian Academy of Sciences - Pázmány Péter Catholic University, Budapest, Hungary
[3]Doctoral School of Mental Health Sciences, Semmelweis University, Budapest, Hungary
[4]Center for Behavioral Brain Sciences, Otto-von-Guericke-Universität, Magdeburg, Germany
[6]Cognitive Biology Group, Institute of Biology, Otto-von-Guericke Universität, Magdeburg, Germany
[5]Department of Psychiatry and Psychotherapy, Semmelweis University, Budapest, Hungary
[7]Institute of Cognitive Neuroscience and Psychology, Research Centre for Natural Sciences, Budapest, Hungary

February 2021

Abstract

Choosing between alternatives is the stuff of everyday life. Many choices require trades between competing objectives, such as between capitalizing on past experience ('exploitation') and updating this experience ('exploration'). In visual perception, where speed is important, there are tensions between stability of appearance, sensitivity to visual detail, and exploration of fundamental alternatives. Presumably, a 'sweet spot' balancing these objectives attains the highest degree of adaptive function. Here, we employ a no-report binocular rivalry paradigm combined with stochastic dynamic modeling to estimate how the visual system balances the objectives of stability, sensitivity, and exploration throughout the lifespan. Observed and simulated results reveal characteristic age- and sex-specific developmental and maturational lifespan trajectories that quantify important aspects of our neurocognitive phenotype. As we also reveal aspects of atypical development underlying mental health disorders, our cognitive modeling may inspire the field of developmental computational psychiatry, in addition to developmental and evolutionary cognitive neuroscience.

1 Introduction

An 80-year-old grandmother and her 8-year-old grandson will react very differently to the same stimulus, e.g., a noisy car approaching. The child will be engaged by the sound, will turn his body in the direction of the sound-source, and drop all the toys he was playing with. On the other hand, grandma has heard this sound so many times, she does not even lift her eyes from the page she was reading. While the child cannot help being over-sensitive to novel stimuli even if he was busy with doing something else, grandmother – relying only on her extensive past experience – is a bit indifferent. The baby's mother would probably just take a quick look to see if there is anything interesting, and continue her ongoing activity. This scenario illustrates the main hypothesis of the paper: adaptive human functioning balances conflicting objectives, and this balance may change throughout life.

Human neurocognitive development is a multidimensional and ever-changing process determined both by biological mechanisms and the environment over the lifespan. Details on the protracted maturation of human structural brain connectivity are emerging with the advance of brain imaging technology [1–5]. It is becoming increasingly clear from such findings that lifespan trajectories of brain organization improve our current, fragmented view of human development. Nonetheless, little is known about the trajectories of active neurocognitive adaptation to the environment, in other words, about the lifetime development of our own behavioural phenotype.

Because of the aforementioned complexity of human growth, the description of the neurotypical behavioural phenotype ought to be complex as well. It does not seem meaningful to ask what the typical brain structure of an adult human is. One needs to specify at least age and sex, since the brain is continually reorganizing, with its development extending into adulthood [6, 7] and as its structure shows differences between the sexes throughout development [8–10]. Adolescence, in particular, is a period of substantial changes in brain structure – notably, in the association cortex, connectivity is remodeled [11], while cortical shrinkage and myelination are accelerated [12,13]. These organizational changes are coupled with a high vulnerability to mental health disorders [14,15]. Parallel to the changes in the brain's structural organization that take place across the lifespan, we should expect changes in the way it adapts to the environment. Further differences should be expected in the case of atypical development underlying mental health disorders, whether resulting from developmental conditions, environmental factors, or a combination of both.

Here, we aim to provide lifetime developmental and maturational trajectories of relevant neurocognitive variables. To this end, we model human visual function as a stochastic dynamics balancing partially conflicting performance measures. We label these measures "stability", "sensitivity", and "exploration", in analogy to concepts from reinforcement learning [16, 17].

In a volatile environment that continually changes in unpredictable ways, a successful interaction must take into account several inherent tensions. For example, relying on past experience in order to make choices in perception or action typically creates an "exploration-exploitation-dilemma" [17–19]. Here, the benefit of safe choices capitalizing on past experience (exploitation) must be weighed against the potential benefit of risky choices flouting precedent (exploration) in order to extend or update this experience. Further tensions arise

when a "cost of time" creates an urgency for reaching timely decisions [20–22]. For example, visual perception generates transiently stable interpretations of continuous sensory input and updates these interpretations at short intervals. Here, the benefit of remaining committed to an interpretation until analysis is complete must be weighed against the benefit of promptly overturning this interpretation in response to ongoing changes in the input. This tension reflects the competing objectives of perceptual stability and sensitivity [22, 23].

We hypothesize that, during the developmental maturation of the human brain, the balance between stability and sensitivity, or between exploitation and exploration, might shift according to developmental constraints. We further assume that reaching an optimal balance, or "sweet spot", might ensure peak adaptive function, probably around the early twenties. Important questions follow from this hypothesis. For example, is the sweet-spot displayed at around the same time for females and males? Is the optimal balance retained, lost gradually, or lost abruptly after reaching the peak? In other words, what are the life-time trajectories of the two sexes in terms of trading stability for sensitivity, and vice versa? As developmental conditions do not always provide for optimal functioning, it is also among our goals to see whether atypical development is accompanied by missing the sweet-spot and knocking the developmental trajectory outside of the typical regime.

Multistable perception, where the perception of an ambiguous sensory input reverses continually between alternative interpretations, offers an attractive paradigm for studying trade-offs between competing perceptual objectives. Multistable perception represents a spontaneous reassessment of perceptual decisions, even when sensory input remains unchanged [24, 25]. Certain characteristics of multistable perception strengthen this notion; notably, the fidelity of evidence for, and ecological likelihood of interpretations, as well as auxiliary information, behavioural context, and prior experience affect the dominance and suppression of interpretations [26], suggesting an underlying inferential process. Observed individual differences in multistable perception – as found across age [27–32], and in multiple psychiatric disorders, such as autism spectrum disorder [33–37] among many others [38–44] – might be assumed to reflect differences in the underlying inferential processes.

In this work, we assess life-time behavioural phenotypes employing multistable perception and dynamic modeling to estimate how the visual system balances the dual objectives of stability and sensitivity. To reach this goal, we measure and model the stochastic dynamics of visual perception under binocular rivalry, a form of multistable perception where different stimuli are shown to each eye. We measure binocular rivalry in a no-report paradigm, which establishes perceptual dominance objectively, purely from eye movements, avoiding confounding cognitive functions related to conscious reporting [45]. Participants viewed two stimuli dichoptically through a mirror stereoscope, while we tracked their left eye's movements (Fig. 1). The stimuli were horizontally moving gratings, which elicit optokinetic nystagmus (OKN), with slow phases (pursuits) in the direction of the stimulus that is consciously perceived at the time [45–47]. Our method of analysis reliably and accurately reproduces perceptual dominance from these slow pursuits [48]. From the observed data, we calculated what parameters describe the participants' behaviour in a dynamical systems model of multistable perception [49]. Given these parameters, we then performed extensive simulations with modulated input to examine how observers

would perform in a volatile environment. We describe this predicted perceptual performance of observers in terms of the partially conflicting performance parameters of stability, sensitivity, and disposition for exploration.

To draw lifespan trajectories of perceptual performance, we conducted the binocular rivalry experiment with a large group of neurotypical participants (N=107) of different ages, from 12-year-old children to senior adults. We chose this broad range of ages to capture the expected developmental changes during adolescence, and follow up the developmental trajectories through adulthood, into senior age. Then, to explore how atypical perceptual performance relates to typical trajectories, we conducted the experiment with two psychiatric groups. One group consisted of young adults diagnosed with borderline personality disorder (BPD; all females) which is associated with developmental vulnerability factors, it is diagnosed predominantly in females [50] (although one study suggests equal prevalence among men and women in the general population [51]), and it is found in adolescents as well as in adults [52]. The second group consisted of young adults diagnosed with autism spectrum disorder (ASD; all males), an early onset neurodevelopmental disorder, more often diagnosed in males [50]. While patients with ASD are known to show alterations in multistable perception [33–37], to our knowledge, there are no studies demonstrating this in BPD. Although atypical sensory perception is not included in the core symptoms of BPD, patients show emotion-related misattributions in the perception of emotionally ambiguous faces (i.e., for faces showing no, or neutral emotion [53, 54]). We hypothesized that patients with BPD would also show atypical behaviour in an ambiguous perceptual situation with more general, non-emotional stimuli. For both ASD and BPD, we expected measures of perceptual parameters to deviate from typically developing subjects.

We found that females and males have different developmental trajectories in terms of the observable variables of binocular rivalry statistics. We calculated a maturation index from these variables, and found that females peak earlier in the maturation index than males. From simulated experiments with modulated input, we found that perceptual performance trajectories also differ in females and males. Females seem to gain in all three perceptual parameter values of stability, sensitivity, and exploration during adolescence, reach a sweet-spot in their early twenties, and remain near the sweet spot until menopause. Males, on the other hand, have their highest values of sensitivity and exploration in early adolescence, both parameter levels decreasing through adolescence. Stability increases until the mid-twenties, and drops continuously after that. The characteristic divergence between the female and male trajectories raises the possibility that the fine-tuning of perceptual function is correlated with sex hormone levels throughout the lifetime. Experiments with the psychiatric patient groups show that their measures (both in terms of binocular rivalry observables, and performance in simulations with modulated input) fall outside of typical maturational trajectories. Overall, our results suggest that the processes underlying perceptual decisions develop across the lifespan, follow a different developmental strategy between the sexes, and are affected by atypical development, resulting either from a developmental condition in the case of ASD, or from a mental illness associated with both genetic and environmental risk factors in the case of BPD.

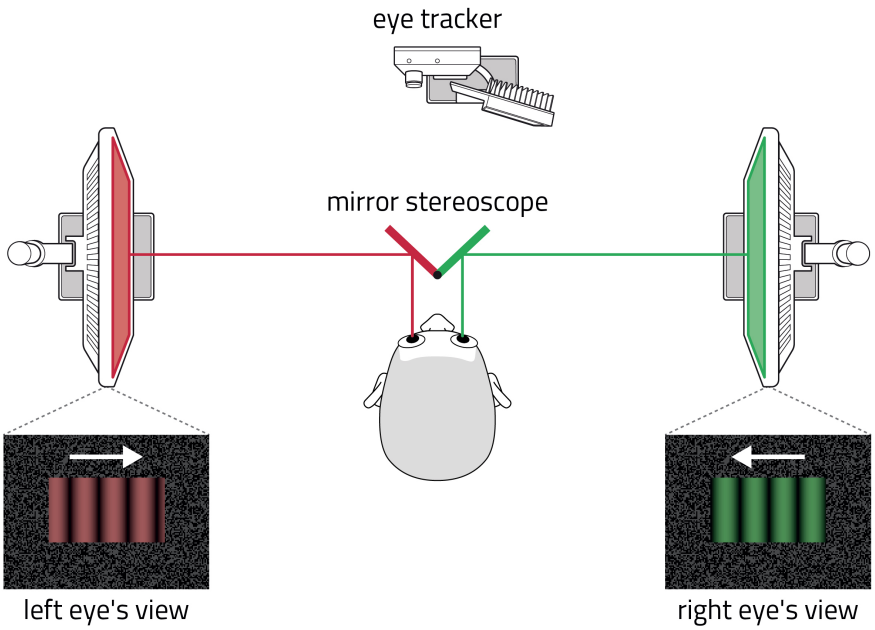

Figure 1: Binocular rivalry paradigm. Participants sat in a mirror stereoscope and viewed two separate displays with their left and right eyes. Displays showed gratings of different colour (red and green) and opposite motion, inducing occasional reversals of phenomenal appearance (binocular rivalry). Perceived appearance and its reversals were monitored objectively by recording optokinetic nystagmus of one eye (OKN), using an automated analysis [48]

2 Results

2.1 Females and males show different developmental trajectories of binocular rivalry dominance statistics

The stimuli in the binocular rivalry experiment consisted of horizontally moving gratings, which differed in colour (red-and-black or green-and-black), and in direction of movement. Such stimuli invoke optokinetic nystagmus (OKN) in the direction of the one currently dominant in perception, allowing for a no-report paradigm, where dominance- and transition periods are extracted from eye movements [47, 48, 55]. Participants viewed the stimuli for ten trials, nine of which were analyzed, each trial lasting 95 seconds. We first conducted the experiment with neurotypical subjects. In this group, a total of 21 typically developing children (12 twelve-year-olds, 19 sixteen-year-olds), and 52 neurotypical adult participants (aged 18-69) took part in the experiment (see Methods for details).

We established the statistics of perceptual dominance periods from the recorded eye movements with an automated OKN analysis [48]. Fig. 2 a, b shows the median duration, interquartile range (IQR), and medcouple (MC, a robust measure of skewness) of dominance period distributions, separately for female and male observers, computed with a log-normal weighted sliding average. The resulting trajectories show considerable difference between sexes, e.g. in terms of the starting and turning points, end points, or in terms of the curved segments of the trajectories. It is noticeable that the direction of the trajectory of female observers changes between the ages of 40 and 50 years, while there is no such second direction change in male observers at a later age.

2.2 Females peak earlier in maturation index derived from dominance statistics

To better summarize the development of the three parameter terms, we obtained a maturation index (MI), shown in Fig. 2 d, by converting all values (from both sexes) to z-scores, applying principal component analysis, and projecting mean parameter triplets onto the first principal component (PC) axis. The first PC accounts for most (79%) of the variance in the data, thus MI provides a good measure of overall differences in dominance statistics. In terms of MI, females peak at an earlier age (age 18.9) than males (age 23.7). The projection of mean parameter triplets on the second and third PCs (which account for 16%, and 3% of the variance, respectively), show smaller modulating effects (Fig. 2 e, f).

2.3 Different trajectories in terms of a dynamic model of multistable perception

To uncover the dynamics underlying the results above, we calculated what parameter values reproduce the observed dominance statistics in a model of multistable perception. We used a model based on the dynamic interaction of competition, adaptation, and noise [23, 49] (Fig 3. a, b). Four model parameters are most consequential in determining dominance statistics: strength of competition (β), adaptation strength (ϕ_a), noise (σ_n) (all relative to input strength, which we set to equal values $I_{1,2} = 1$), and the time-constant of adaptation

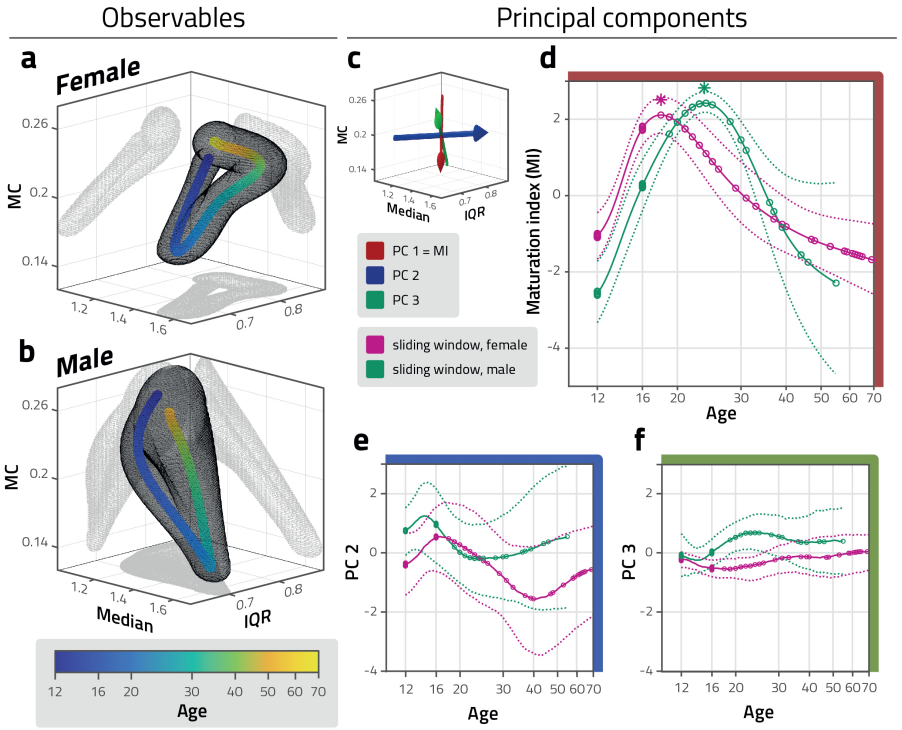

Figure 2: Developmental and maturational trajectory of distribution parameters. a, b: Parameters of distribution of dominance durations – median duration (median), interquartile range (IQR), and medcouple (MC) – during development and maturation of neurotypical female and male observers (blue to yellow color scale). The grey mesh represents mean values ± 50% SEM, computed with sliding log-normal weighting and repeated sampling with replacement. The developmental trajectories of the two sexes differ notably within this space. c: Principal component (PC) axes of mean distribution parameters observed over all ages and sexes (computed after conversion to z-score values). First (red), second (blue) and third (green) components account for 79%, 16%, and 3% of the variance, respectively. A maturational index (MI) is obtained by projecting mean parameter triplets onto the first principal component axis. d: Maturation index (MI) of neurotypical female and male observers (magenta and green, respectively), as a function of age. At age 18.9 and 23.7, peak values of 2.11 and 2.42 are reached by female and male observers, respectively (stars). Sliding window average (solid curves) and confidence intervals (±100% SEM, dotted curves) in harmonized units (z-score values). Individual observers are also indicated (circles). e, f: Development and maturation along second (e) and third (f) principal component axes, in harmonized units (z-score values). Note far smaller variance with age compared to (d).

(τ_a). We performed the calculations with four different, fixed levels of competition strength: $\beta = 1$, $\beta = 2$, $\beta = 3$, and $\beta = 4$ (in what follows, results are illustrated with $\beta = 3$). Other, less consequential parameters were also fixed (time-constants of activity τ_n and noise τ_r, inflection point of activation function k; see Methods). We systematically varied ϕ_a, τ_a, and σ_n to reproduce the experimentally observed mean dominance distribution parameters, within a $\pm 5\%$ tolerance limit (see Methods for details).

The resulting volumes of model parameters for females and males - in ϕ_a-τ_a-σ_n subspace, with $\beta = 3$ - are shown in Fig. 3 c, d. Both females and males show a similar trajectory in terms of adaptation time constant: an increase in development (from childhood to young adulthood), and a decrease during maturation (from young adulthood to senior age). Distinctly, females develop toward larger values of adaptation strength, and smaller values of noise, while males develop towards smaller values of adaptation strength, and larger values of noise. This reflects a tight trade-off between adaptation and noise in the dynamics of multistable perception - strong adaptation is coupled with small noise, or vice versa, weak adaptation with large noise. During maturation, there is a decrease in adaptation time constant for both females and males. In the female model parameter trajectory, as in that of binocular rivalry dominance, there is a second change of direction between young adulthood and senior age, with an increase in noise. There is no similar change of direction seen in the male trajectory.

2.4 Simulations in a volatile environment predict different perceptual performance trajectories

The reproduction of dominance statistics revealed that the developmental and maturational trajectories of the mechanisms underlying multistable perception differ notably between females and males. While input biases were treated as equal in the model, this is not the general case when making perceptual decisions, where the environment is changing and uncertain. Thus, we aimed to explore the perceptual performance along development and maturation by predicting the behaviour of observers in a volatile environment, with stochastically changing, unequal inputs. In particular, we wanted to predict and describe the relative contribution of the environment (external state) vs. that of the perceptual system (internal state) in perceptual decisions - in this context, perceptual stability (no change in perceived stimulus) or reversal (change in perceived stimulus).

To accomplish this, we performed simulations, subjecting the fitted parameter models (described above) to a volatile environment with a stochastically changing input bias ΔI. This parameter describes the volatility of the environment, i.e., the external state. The model's state variables r_1, r_2 (responses) and a_1, a_2 (levels of adaptation) change dynamically and stochastically in response to this environment (Fig. 4 a). Variables r_1 and r_2 are most of the time binary (near zero or near unit value), taking intermediate values briefly during transition periods around reversals (time points where $r_1 = r_2$). Variables a_1 and a_2, on the other hand, change gradually - this may be summarized as the time varying adaptation bias Δa $(a_1 - a_2)$. Together, the joint statistics of input bias, i.e. external state ΔI, model response, i.e. internal state Δa, and the occurrence of reversals characterize the perceptual performance of the model in

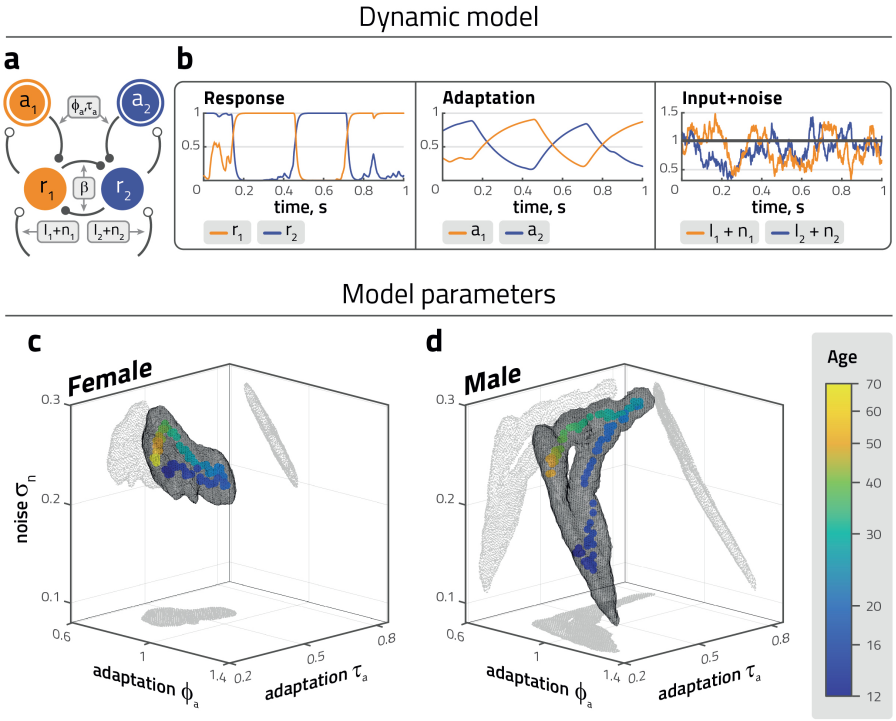

Figure 3: Development and maturation of fitted model parameters. a: Dynamic model of binocular rivalry, with competition, adaptation, and noise. Two representations (r_1, r_2) are driven by associated visual inputs (I_1, I_2) and independent noise (n_1, n_2). Each representation is inhibited by the other, as well as by the associated adaptive state (a_1, a_2). Free model parameters are competition strength (β), adaptation strength (ϕ_a), adaptation time-scale (τ_a), and noise amplitude (σ_n). Input strength is fixed at $I_1 = I_2 = 1$. b: Representative example of model dynamics with abrupt dominance reversals of activities r_1 and r_2, gradual build-up and recovery of adaptive states a_1 and a_2 (middle), and noise n_1 and n_2 added to visual input $I = 1$ ($\beta = 2$, $\phi_a = 0.7$, $\tau_a = 0.3$, $\sigma_n = 0.2$). Reversals may be triggered by differential adaptive state $a_1 - a_2$, differential noise $n_1 - n_2$, or both. c, d: Parameter triplets ϕ_a-τ_a-σ_n fitted to reproduce (within a $\pm 5\%$) experimentally observed mean distribution parameters. Competition strength was fixed at $\beta = 3$. Centroid values (colored dots) and confidence range ($\pm$ standard deviation, gray mesh).

a volatile environment.

After performing the simulations, we distinguished between transition periods (20 ms before and after reversal), initiation periods (40-21 ms before reversal), and all other times in the resulting time-series, in 1 ms intervals (Fig. 4 a). We disregarded transition periods, as they concern the largely stereotypical time course of the reversal itself, rather than the initiation of the reversal. Then, we established how the initiation of reversals depend on external and internal state, by computing the conditional likelihood of reversals as a function of ΔI and Δa values during initiation periods, in the vicinity of the median ΔI and Δa values, $P_{init}(\Delta I, \Delta a)$ (Fig. 4 b; see Methods for details).

We found that in the vicinity of the median state (ΔI_m, Δa_m), the logarithm of initiation probability $\log P_{init}$ varies almost linearly with state variables ΔI and Δa (quality of linear regression $r^2 > 0.99$). As this planar dependence has three degrees of freedom, it can be described in terms of three parameters of perceptual performance: sensitivity, exploration, and stability. (Fig 4 b, c) Sensitivity, the maximal gradient of $\log P_{init}$ with respect to state variables ΔI and Δa, defined as the length of the gradient vector $\partial \log P_{init}(\Delta I,\ \Delta a)$ at the median state, measures how rapidly $\log P_{init}$ changes with state (ΔI, Δa). Exploration, the direction of the gradient vector at the median state, measures the relative influence of internal state Δa, compared to external state ΔI, on the log conditional likelihood of reversals, $\log P_{init}$. And stability, the difference between $\log P_{init}$ at the median and the neutral state (defined as $\Delta I = \Delta a = 0$), measures the stabilizing or destabilizing effect of the median state. For positive values of stability, median state lowers reversal probability, i.e. stabilizes the percept. For negative values of stability, the opposite is the case, i.e. the median state destabilizes the percept. (For more details, see Methods.)

The values of stability, sensitivity, and exploration, derived from the volatile-environment simulations on the fitted model parameters of neurotypical observers, are shown in Fig. 4 d, e. While the developmental and maturational trajectories have some similarities, they differ notably between sexes.

Females gain higher values of stability, sensitivity, and exploration during development, and reach peak values at young adulthood, which then decreases slowly during maturation. Males, on the other hand, have peak values of sensitivity and exploration at an early age. They gain stability during development, which peaks at young adulthood, but at the same time lose sensitivity and exploration. This shows different developmental strategies between sexes, in which females gain in all three measures of stability, sensitivity, and exploration during adolescence, while males have higher values of sensitivity and exploration in early adolescence, which decrease during adolescence, coupled with an increase in stability.

2.5 Clinical populations fall outside of typical developmental and maturational trajectories

In addition to neurotypical observers of various ages, we performed the same set of procedures - binocular rivalry experiment, model fitting, and volatile-environment simulations - with two adult clinical groups: 12 females with borderline personality disorder (BPD; mean age 27.1), and 12 males with autism spectrum disorder (ASD; mean age 28.5). The observed binocular rivalry dominance distribution parameters, and predicted perceptual parameters are shown

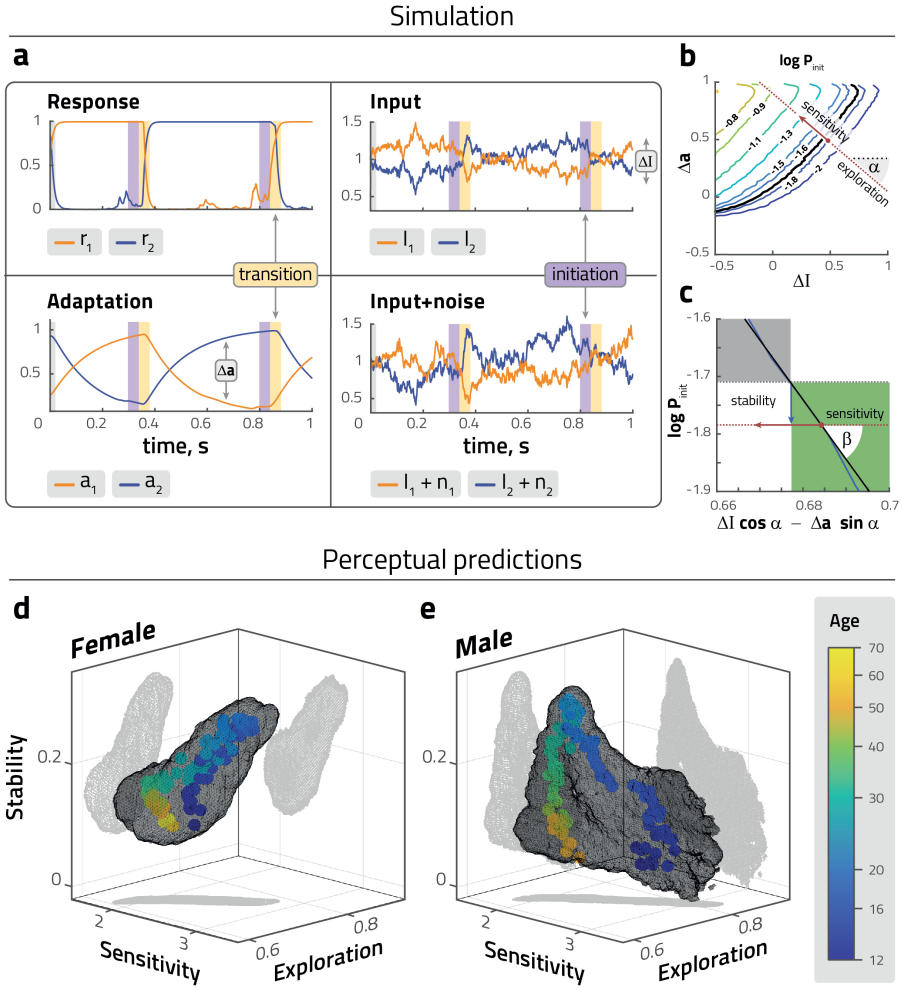

Figure 4: **Predicted perceptual behaviour in a volatile environment.** a: Representative example of simulated dynamics of fitted model: activities r_1, r_2 and adaptive states a_1, a_2 driven by intrinsic noise n_1, n_2 and variable sensory inputs I_1 and I_2. In a volatile environment, reversals (defined by $r_1 = r_2$) may be triggered externally (differential input $\Delta I = I_1 - I_2$) or internally (differential adaptive state $\Delta a = a1 - a2$) or both. To assess reversal initiation, we distinguished between transition periods (yellow stripes, 20ms before and after $r_1 = r_2$), immediately preceding periods (purple stripes, 40 to 21 ms before $r_1 = r_2$), and all other times. b: Based on this classification, we computed the conditional likelihood of reversals (colored contours) as a function of ΔI and Δa values during initiation periods, in the vicinity of the median ΔI and Δa values (over all periods, red dot). In this vicinity, the reversal probability grows exponentially in a particular direction (red dashed line). The length of the gradient vector $\partial \log P(\Delta I, \Delta a)$ represents the 'sensitivity' of reversal probability to ΔI and/or Δa values, and the 'exploration' angle α represents the relative influence of internal state Δa, compared to external state ΔI (external state). A larger value implies that the system responds less consistently to external state, behaving in a more explorative manner. c: Enlarged cut through the $\log P(\Delta I, \Delta a)$ surface in the direction of the the gradient vector (red arrow), showing the neutral level (defined by $\Delta I = \Delta a = 0$, black dashed line) and median level (red dashed line). The distance between levels (blue arrow), represents 'stability' and measures the stabilizing or destabilizing effect of external and internal median states. For positive values (within green area), median states lower reversal probability, stabilizing the percept; vice versa for negative values (within grey area). d, e,: Developmental and maturational trajectories of predicted perceptual parameters (stability, sensitivity, exploration) for females (d) and males (e). Mean values (coloured dots) and confidence intervals (standard deviations, grey volumes).

in Fig 5, contrasted with the corresponding sex's typical developmental and maturational trajectories (results of the model fitting are shown in Supplementary Fig. 1).

The results show that both atypical groups fall outside the typical developmental and maturational trajectories. Despite the different character of their respective disorders, they differ from the typical trajectories in similar ways. In terms of observable dominance distribution parameters (Fig. 5 a, b), both groups show lower median and IQR, and higher MC values. In the predicted perceptual performance in a volatile environment (Fig. 5 c, d), both groups have higher values of sensitivity and exploration, compared to neurotypicals.

3 Discussion

The perceptual parameters predicted by our model are broadly analogous to competing objectives prescribed by the framework of reinforcement learning. When objects can appear or disappear at any time, the thoroughness of object classifications must be balanced against the frequency of such classifications [20, 21]. In our context, this corresponds to a balance between stability (temporal persistence of current choice) against sensitivity (susceptibility to changed circumstances, internal or external) [22, 23]. Additionally, in an unstable world the value of past experience diminishes with time, so that the benefit of past experience must be weighed against the benefit of discovering something new (exploitation-exploration dilemma [17–19]). In our context, this corresponds to the weight afforded to external states (input bias), relative to internal states (adaptation bias) that prompt a fundamental reassessment of such evidence. Hence the relative weight of adaptation bias represents a tendency for exploration.

The main purpose of our study was to draw lifespan trajectories of perceptual performance in both neurotypical and psychiatric populations. With respect to neurotypical brain development and maturation, our results indicate that visual decision making, assessed in a multistable perceptual paradigm, changes markedly in adolescence, and then more gradually across the lifespan. We found sex-specific lifetime maturation trajectories suggesting that biological maturation plays a major role in visual decision making. Neuroendocrine changes, especially the levels of sex steroid hormones are known to time bodily growth, emotional development and cortical pruning in adolescence [5, 56, 57], and seem to influence cognitive function during [58,59] and after the teenage years [60,61]. The fact that females peak earlier (around 19 years of age) than males (around 24 years of age) in maturation index in our study is in line with the known delay of puberty onset times in boys as compared to girls [62] and the relatively late peaks indicate a neotenous human-specific function, involving the latest maturing brain areas such as the prefrontal cortex and the precuneus [63, 64].

The perceptual performance trajectories predicted by our simulations provide further details on the specific parameters determining development and maturation. The trajectories of neurotypical females and males also demonstrate marked age- and sex-specific variations. Males are going through an uninterrupted change after the apex in young adulthood, while the trajectory has a second abrupt turn of direction in females around the time of menopause. This second inclination in the perceptual performance trajectory might be the

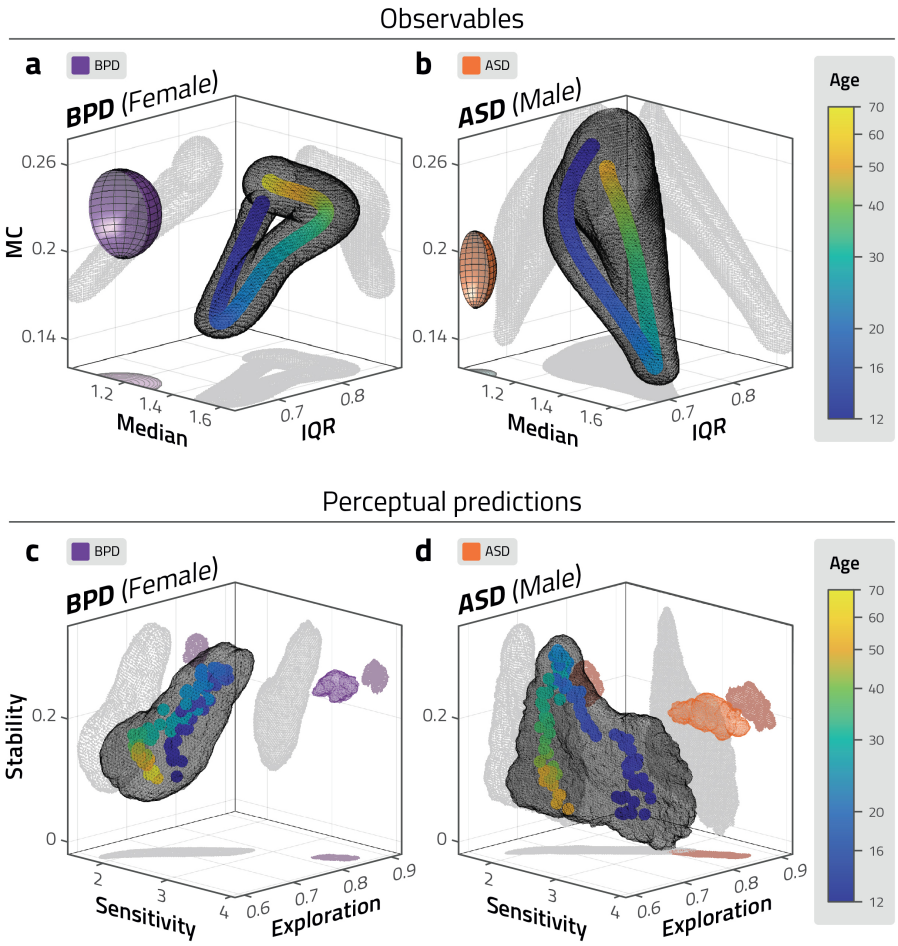

Figure 5: Observed distribution parameters and predicted perceptual behaviour of atypical groups. Observed distribution parameters (a, b), and predicted perceptual behaviour in volatile environments (c, d) for atypical groups, compared to neurotypical trajectories. Observers with borderline personality disorder (BPD, all female) are compared to neurotypical females of different ages. Observers with autism spectrum disorder (ASD, all male) are compared to neurotypical males of different ages. (a, b) Ellipsoids represent mean SEM values for BPD (purple) and for ASD (in orange). (c, d) Coloured volumes represent confidence intervals (standard deviation) for BPD (purple) and for ASD (in orange). The dominance period statistics and perceptual predictions of both groups fall outside the typical developmental and maturational trajectory.

consequence of a sharp gonadal hormone falloff later in life in females [65], while the gradual change might be reflecting the progressive decline of sex hormones in males [66].

In terms of perceptual parameters estimated by our model, females are characterised by increasing values of stability, sensitivity, and exploration during adolescent development. Peak values of all three parameters are reached by twenty, defining a sweet-spot of optimal function for perceptual decisions. After the peak, a moderate decline can be observed until menopause, which is similar in all three parameters. Signs of a stability-sensitivity trade-off can be observed after menopause when stability declines sharply, with slight increases in sensitivity and exploration, following the male pattern in this age-group. Males, on the other hand, have peak values of sensitivity and exploration by the age of sixteen, exceeding the highest female levels. The heightened sensitivity is coupled with extreme low levels of stability, demonstrating a clear trade-off between these parameters that might show up so distinctly only in the higher parameter ranges. Until the mid-twenties, stability rises at the expense of sensitivity and exploration. The male sweet-spot of optimal function seems to be characterised by lower sensitivity and exploration levels, but a higher level of stability as compared to females. After the peak, males decline progressively in stability. This intriguing and complex pattern in the lifespan evolution of the two sexes demonstrates, on one hand, that the rules of growth are not uniform even in the developmental period, and on the other hand, it clearly shows that ageing is not simply the "reverse" of development as it has been suggested with respect to other cognitive functions as well [67], even though, to our knowledge, such a detailed pattern of later development has not been described before.

Given the obvious biological determination reflected in the age- and sex-specific differences, we interpret this pattern of findings as a result of alternative developmental strategies. It seems that females approach the peak in all three parameters faster, and although this provides them with lower peaks as compared to males, it also seems to provide for a greater stability throughout the childbearing years, with a major decline only after menopause. The trade-off between stability and sensitivity is more obvious in males who start with maximum levels of sensitivity and exploration mid-adolescence, and in parallel to stability building up by the mid-twenties, a great deal of sensitivity is lost. The greater exploration range in the early years, the higher apex, and the continuous decline after the apex might indicate a developmental strategy to fine-tune the individual for the age of highest fertility in males [68]. Although sex-difference research cannot always escape design flaws and misinterpretation, we believe that our carefully collected and analysed data-set reveals biologically grounded cognitive differences between the sexes without the indictment of "neurosexism" [69]. These alternative developmental strategies - one focusing on stability throughout the childbearing period, and the other, focusing on highest performance by the peak fertility age - are particularly interesting in the context of perceptual decisions. Decisions made between alternatives, even if not volitional or highly conscious, make up our everyday life, and the particular style with which we are dealing with those decisions will, in fact, determine our life. It makes a difference, for example, whether our brain is tuned to be relatively insensitive to environmental changes, rendering decisions stable and stereotypical and preventing extensive exploration or, in another scenario, whether higher sensitivity is combined with a heightened inner drive for exploration. In the first

case, we might function with high stability and acceptable sensitivity in a manner that provides for our offspring, whereas, in the second case, we might forgo stability and explore with high sensitivity in a manner that procures optimal mates for reproduction. At this point, we can only speculate that there is indeed a direct link between gonadal hormone levels and perceptual performance throughout the lifetime, and further investigations into this issue are definitely due. However, the pattern in our data seems to be very compelling, and suggests that age- and sex-specific variations should not be overlooked when testing psychological function.

After obtaining such fine-resolution developmental and maturational lifetime trajectories of neurotypical subjects, it is of particular interest how these would be drawn when biological conditions or environmental factors are not adequate for typical development. To this end, we have tested two psychiatric groups: adult participants with borderline personality disorder and with autism spectrum disorder. In terms of our measures, the perceptual parameters of these patient groups (all males for ASD, and all females for BPD) fell completely outside of the typical developmental trajectories for their respective sex – i.e., adults with these disorders differed not only from neurotypical adults of a similar age, but from the measures of any examined ages, probably missing the sweet-spot of optimal function at an earlier age. In terms of the trade-off, both patient groups demonstrate sensitivity and exploration levels beyond the range of neurotypical, while stability is reduced markedly only in males, resembling the pattern seen in neurotypicals. As all psychiatric patients in the study were adults, we cannot pinpoint the when-and-how of the deviations from typical trajectories in ASD and BPD from these results. It is likely that the onset of deviations is present from early childhood in ASD as sensory symptoms and differences in visual perception are already present in childhood [70], and multistable perception already differs from that of typically developing children before adolescence [36]. Since BPD is not characterised as a neurodevelopmental disorder, deviations probably have a later onset. By adolescence, the disorder can be reliably diagnosed [52], so the deviations from typical trajectories likely occur during, or somewhat before, adolescence.

In interpreting the clinical findings, it should be mentioned that BPD is a disorder that predominantly affects females [50] (but note that a study found equal prevalence of BPD among the sexes in the general population [51]). Distinctive patterns in hormone levels, especially the relative changes in ovarian hormones may induce the expression of BPD features [71]. Our BPD participants seem to be in a much higher sensitivity and exploration range than neurotypical women of the same age, however, this is obtained at the expense of stability, demonstrating the force of the trade-off, especially outside of the sweet-spot. In the light of our neurotypical results and the particular hormonal impact on the psychopathology of BPD, it is in our future plans to include hormonal assessments in the toolkit of the current study.

With respect to ASD which is more often diagnosed in males [50], a similar tendency can be observed: increased levels of sensitivity and exploration and reduced stability as compared to neurotypicals of similar age. Although female under-diagnosis [72] should not be overlooked, a popular theory of autism claims that the autistic brain is a hypermasculinized version of the male brain due to increased fetal testosterone levels [73]. In terms of excessive levels of sensitivity and exploration, our result supports this picture, although alternative interpre-

tations, such as a general drawback of sex differentiation [74,75] cannot be ruled out. Including female ASD participants, and hormonal assessments would be essential in further studies.

Our results regarding ASD and BPD may inform the field of computational psychiatry, which aims at the large-scale phenotyping of human behaviour using computational models, with the hope that it may structure the search for genetic and neural contributions of healthy and diseased cognition [76]. Within this field, the framework of developmental computational psychiatry aims to establish normative developmental trajectories of computations, relate them to brain maturation, and determine when and how they deviate in mental disorders, in order to help uncover the relationship between the changes of brain organization in childhood and adolescence, and the heightened vulnerability to psychiatric disorders in these periods [15]. Our results fit into this framework by establishing typical developmental trajectories of visual decision making, and relating results from subjects with mental disorders to these trajectories. They also may serve as a small step of the large-scale phenotyping efforts to better understand the nature of mental disorders in terms of aberrant computations.

Since we did not employ any neuroimaging methods in this study, we can only speculate about the changes of brain structure underlying the observed developmental and maturational trajectories. While the overall structure, organization, and connectivity of the brain is established by birth, important changes take place in later development in structural brain connectivity [1–5], with known differences between the sexes [8–10]. Our results roughly follow the course of the described overall structural changes, although beyond the teenage years, maturation is reflected more in the specialization of the brain than in anatomical growth [77]. The specialization of neural systems results in a shift from local to distributed connectivity profiles (i.e., short range networks weaken, while long-range networks strengthen), changes in the strength of specific networks, and in the hierarchical modular structure of networks, e.g., in the brain's hub structure [78]. The long-range pliability of the brain both in terms of connectivity is coupled with prominent vulnerability to mental disorders [14,15]. In ASD, studies examining functional connectivity have heterogeneous results with converging evidence, suggesting global under-, and local overconnectivity of the brain, supporting a theory of less segregation within functional networks, and more diffuse connectivity between some networks in ASD [79]. A recent study suggests that the macroscale cortical hierarchy is disturbed in ASD, with reduced functional distance between the sensory areas and unimodal convergence regions at one end of the hierarchy, and transmodal association cortices on the other [80]. Results of both under- and over-connectivity in different regions are reported in BPD [81], with a study showing, among other alterations in network connectivity, higher connectivity within some non-hub nodes, and decreased connectivity at several hub nodes [82]. The connectivity of hub regions in the association cortex, which is remodeled in adolescence [11], and some of which show decreased connectivity in the observed psychiatric disorders, may be a potential link to connect our results of marked developmental changes in adolescence, and the similarly-differing atypical results in ASD and BPD.

To conclude, in our detailed study on the lifespan trajectories of perceptual performance employing a no-response binocular rivalry paradigm combined with dynamic computational modeling, we have found characteristic age- and sex-specific developmental and maturational trajectories, with marked differences

between neurotypical and psychiatric populations. These trajectories should serve to better describe our own neurocognitive phenotype and reveal relevant factors behind atypical development underlying mental health disorders.

4 Methods

4.1 Participants

A total of 107 participants took part in the binocular rivalry experiment: 28 twelve-year-old (19 female), and 19 sixteen-year-old (10 female) children; 52 neurotypical adults (average age 35.9, range 18 to 69, 32 female); 12 adults with autism spectrum disorder (ASD, average age 29, range 19 to 44, n=12, all male), and 12 adults with borderline personality disorder (BPD, average age 27, range 20-37, n=12, all female). Participants were considered typically developing, or neurotypical, if they reported no history of mental illness or disorder.

Nine of the twelve participants with ASD were recruited from the Department of Psychiatry and Psychotherapy, Semmelweis University. These participants were diagnosed by a trained psychiatrist. They went through a general psychiatric examination, and their parents were interviewed about early autism-specific developmental parameters. All participants fulfilled the diagnostic criteria of ASD, including autism-specific signs between the ages of 4-5 years. The other three participants in this group were recruited from Aura Organization, a nonprofit organization assisting people with ASD. We did not collect further diagnostic information from these participants. The participants with BPD were all recruited from the Department of Psychiatry and Psychotherapy, Semmelweis University. Their diagnostic status was assessed by the Hungarian version of the Structured Clinical Interview for the Diagnostic and Statistical Manual of Mental Disorders, fourth edition, Axis I and II disorders.

All participants had normal or corrected to normal vision, and reported no colour blindness. Before the experiment, all participants passed a stereoacuity test (Super Stereoacuity Timed Tester, by Stereo Optical Co., U.S. Patent No. 5,235,361, 1993). All adult participants, and all the children's caregivers have provided informed written consent. The study was approved by the Ethical Review Committee of the Institute of Psychology, Pázmány Péter Catholic University for neurotypical participants, and by the Semmelweis University Regional and Institutional Committee of Science and Research Ethics for participants with a psychiatric condition. Participants were given a book voucher for their participation.

4.2 Binocular rivalry experiment

Participants were fixated at a headrest during the experiments (SR Research Head Support, https://www.sr-research.com). The setup for dichoptic stimulation consisted of two LCD displays (subtending 26.6° horizontally and 21.5° vertically, with an approximate resolution of 48 pixels/° of visual angle, and a refresh rate of 120 Hz), which participants viewed through two 45° mirrors, attached to the headrest. The mirrors were coated, such that they reflected the visible light spectrum, but transmitted infrared light, allowing the use of an infrared camera for optical eye tracking.

The participants viewed green-and-black gratings with one eye, and red-and-black gratings with the other eye. The gratings moved horizontally, either consistently (in the same direction), facilitating perceptual fusion, or inconsistently (in opposing directions), facilitating perceptual rivalry. Each grating subtended a rectangular area of 15.2° width and 8.4° height. The spatial frequency was 0.26 cycles/°, and the temporal frequency 8.7 cycles/s. The motion's speed was 33.5°/s or 1600 pix/s. Gratings were framed in a rectangular box with a random texture pattern, in order to facilitate binocular fusion. Stimuli were generated with Psychophysics Toolbox 3 [83–85] running under MATLAB R2015a. The display's spatial resolution was 48 pix/°, and its temporal refresh rate was 120 Hz.

Before the experiment, participants were asked to view the display as attentively as possible, and to follow the horizontally moving gratings with their gaze. This was introduced with analogies such as "follow them like you would follow passing trees on a moving train". We did not tell them that they will see rivalling stimuli, only that if the direction of the gratings they see will seem to change, let their gaze change direction too. We asked them to refrain from blinking as much as convenient. Participants did not have to report which stimuli they were perceiving at any time. Instead, perceptual states and transitions were calculated from eye-movement recordings.

The experiment consisted of ten trials, each 95 s long. The initial trial (introductory trial) served to familiarize participants with the display, and was not included in the analysis. It started with 22 s of consistent grating motion in alternating directions, followed by 72 s of inconsistent motion, and finishing with 1 s of consistent motion. During the introductory trial, we provided feedback for the participants on the behaviour of their eye movements. The following nine trials (experimental trials) began with 2 s of consistent motion, followed by 92 s of inconsistent motion, and ended with 1 s of consistent motion. The consistent episodes served to reduce eye strain and to test the ocular response to physical motion reversals. On experimental trials, participants received no feedback on their behaviour. Across trials, the colour (either red or green) and direction (either leftward or rightward) shown to each eye was altered. The experiment consisted of three blocks. After the third and sixth experimental trials, participants had a 5-minute break.

4.3 Establishing reversal sequences and dominance statistics from OKN

When a rivalrous display induces horizontal OKN, the direction of smooth pursuit phases provides a reflex-like indication of perceived direction [45–47]. During the experiment, we recorded horizontal eye position of subjects with a sample rate of 1000 Hz, and inferred reversals of perceived direction with the cumulative smooth pursuit (CSP) method, described elsewhere [48]. Briefly, the method removes off-scale values (blinks and other artefacts), and defines slow pursuit segments by a compound criterion (slow velocity $|v| \leq 1.5$ pix/ms, low acceleration $|a| \leq 0.12$ pix/ms^2, duration > 50 ms), aligns slow pursuit segments, interpolates gaps, then subsamples and fits the resulting sequence multiple times ("bagging" [86]). The result of this robust splining procedure is estimated eye velocity (median and 95% CI) at every time-step. Dominance periods were defined as contiguous intervals in which the entire 95% CI is either above or below

a gaze velocity threshold of ±0.1 pix/ms. All other intervals were designated as perceptual transition periods.

As the rate of perceptual reversals often accelerates while viewing a binocular rivalry display [87, 88], the initial 30 seconds of each trial were discarded from analysis. We pooled the remaining reversal sequences obtained for each observer across different trials, and calculated the median (M), interquartile range (IQR), and medcouple (MC) of dominance durations. These robust statistical measures were used to reduce the effect of outliers. Median and interquartile range (IQR) provide robust alternatives for first and second moments (mean and variance), while medcouple (MC) offers a robust alternative for the third moment (skewness), which is particularly sensitive to outliers.

4.4 Establishing developmental and maturational trajectories

For each observer i, three distribution parameters were established as described above: M_i, IQR_i, MC_i, and age a_i. From the individual observer values, average values were computed separately for female and male observers. As development slows down with age, sliding averages were computed with log-normal weighting, so that window size increased proportionally with age. For median M_i, $\overline{M_i}$ was computed as follows:

$$\overline{M_i} = \frac{\sum_j M_j LN(a_j|a_i)}{\sum_j LN(a_j|a_i)}, \qquad LN(a_j|a_i) = \frac{1}{a_j - a_0} \exp[-\ln(a_j - a_0) - a_i + a_0 / 2\sigma^2],$$

where $a_0 = 8$ and $\sigma = 0.35$.

$\overline{IQR_i}$and $\overline{MC_i}$ were obtained analogously. Confidence intervals were computed by repeatedly sampling observers with replacement, and recomputing the average parameters.

4.5 Computing maturation index

As all parameters tended to change concomitantly, we sought to summarize the development of all three parameters in terms of a single maturation index. As a first step, averaged distribution parameters $\overline{M_i}$, $\overline{IQR_i}$, $\overline{MC_i}$ were normalized (z-scored), to obtain values $\widehat{M_i}$, $\widehat{IQR_i}$, $\widehat{MC_i}$ with zero mean and unit variance, over all typically neurotypical observers. Next, we computed the principal component direction over all typical observers (both male and female), which captured most of the variance ($\sim$ 80%). We defined the maturation index (MI) as the projection of normalized average parameters ($\widehat{M_i}$, $\widehat{IQR_i}$, $\widehat{MC_i}$) onto this direction, or equivalently, a linear combination of these parameter triplets:

$$MI = PC1 = 0.542\ \widehat{M_i} - 0.567\ \widehat{IQR_i} - 0.620\ \widehat{MC_i} \qquad (79\% \text{ variance})$$

The maturation index provided a convenient summary of binocular rivalry statistics over different ages and sexes. The other components were:

$$PC2 = 0.765\ \widehat{M_i} + 0.639\ \widehat{IQR_i} + 0.084\ \widehat{MC_i} \qquad (16\% \text{ variance})$$
$$PC3 = 0.349\ \widehat{M_i} - 0.520\ \widehat{IQR_i} + 0.780\ \widehat{MC_i} \qquad (3\% \text{ variance})$$

Confidence intervals were computed by repeatedly sampling observers with replacement, and recomputing the average parameters.

4.6 Computational model implementation

Bistable perception was modeled in terms of a dynamic system with competition, adaptation, and noise. The specific formulation we used was introduced by Laing and Chow [49, 89, 90] and has been analyzed and extended by several other groups [23, 91–94].

The dynamic response $r_{1,2}$ of each neural representations is given by

$$\tau_r \dot{r}_{1,2} = -r_{1,2} + F\left(-\beta r_{2,1} - \phi_a a_{1,2} + I_{1,2} + n_{1,2}\right)$$

with sensory input $I_{1,2}$, intrinsic noise $n_{1,2}$, adaptive state $a_{1,2}$ and activation function

$$F(x) = \left[1 + \exp\left(-x/k\right)\right]^{-1}$$

The dynamics of adaptive states $a_{1,2}$ is given by

$$\tau_a \dot{a}_{1,2} = -a_{1,2} + r_{1,2}$$

and intrinsic noise $n_{1,2}$ is generated from two independent Ornstein–Uhlenbeck processes:

$$\dot{n}_{1,2} = -\frac{n_{1,2}}{\tau_n} + \sqrt{\frac{2\sigma_n^2}{\tau_n}}\xi$$

where ξ is normally distributed white noise. Different dynamical regimes may be obtained by varying competition (β), adaptation (ϕ_a, τ_a), and noise (σ_n), while keeping time constants τ_r and τ_n, and activation parameter k fixed. Inputs were set as equal ($I_1 = I_2 = 1$).

4.7 Fitting computational model parameters

We performed grid simulations for competition strengths $\beta = 1$, $\beta = 2$, $\beta = 3$, and $\beta = 4$, because competition strength is not well constrained by our observations. Each simulation lasted 104 s and covered 100-by-100-by-100 value triplets of the other critical model parameters, adaptation strength (ϕ_a), time constant of adaptation (τ_a), and noise (σ_n). The explored range of parameter values was $\phi_a \in [0.1, 0.5]$, $\sigma_n \in [0, 0.1]$ for $\beta = 1$; $\phi_a \in [0.3, 1.2]$, $\sigma_n \in [0, 0.4]$ for $\beta = 2$; $\phi_a \in [0.5, 2.0]$, $\sigma_n \in [0, 0.4]$ for $\beta = 3$; and $\phi_a \in [1, 4]$, $\sigma_n \in [0, 0.5]$ for $\beta = 4$. For all values of β, τ_a was in a range of $[0.1, 1.3]$ s. The remaining, non-critical parameters were $I_{1,2} = 1$, $\tau_n = 0.1$ s, $\tau_r = 0.02$ s, $k = 0.1$, and $dt = 0.002$ s in all four cases.

For each of the 3-by-106 value quadruplets of β, ϕ_a, σ_n, and τ_a, we parsed the resulting reversal sequence of 104 s duration into dominance periods by taking $sign(r_1 - r_2)$, and calculated three summary statistics of dominance duration: median, interquartile range (IQR), and medcouple (MC).

To compare simulations to the reversal statistics of human observers, we identified combinations of model parameters that reproduce the observed binocular rivalry statistics (median, IQR, MC). Specifically, those parameter combinations were selected for which the simulated median, IQR and MC falls within 5% of the respective mean values obtained for any given participant.

4.8 Simulating experiments with modulated inputs

After fitting model parameter combinations to observers, we performed simulations on these parameter combinations with a time-varying input bias, ΔI_t, generated as an Ornstein-Uhlenbeck process with standard deviation $\sigma_I = 0.3$ and autocorrelation time $\tau_I = 0.2$ s. To keep total input constant $I_1(t) + I_2(t) = 2$, the bias was applied anti-symmetrically $I_1(t) = 1 + \Delta I(t)$, $I_2(t) = 1 - \Delta I(t)$.

The simulated dynamics were obtained in time-steps of 1 ms, and included response $\Delta r = r_1 - r_2$, perceptual dominance $sign(\Delta r)$, differential adaptation $\Delta a = (a_1 - a_2)\ sign(r)$, and differential input $\Delta I = (I_1 - I_2)\ sign(\Delta r)$. Note that positive Δa favours the suppressed percept, whereas positive ΔI favours the dominant percept. Intrinsic noise $n_{1,2}$ was treated as unobservable, and was subsumed in the probabilistic analysis described in the next section. In other words, probabilities and expectation values were obtained by averaging over intrinsic noise.

4.9 Obtaining perceptual parameters

We calculated perceptual parameters from the simulations described above. In the simulated time series, reversals were defined as time-points where responses were equal, $r_1 = r_2$. To calculate perceptual parameters, we disregarded transition periods, defined as 20 ms before and after a reversal. We classified all other time points as either initiation periods preceding a reversal (40-21 ms before a reversal), or as periods not closely preceding a reversal. Based on this classification, we established the following probabilities: the joint probability of $P(\Delta I, \Delta a)$, the conditional joint probability given a subsequent reversal (being in initiation) $P(\Delta I, \Delta a \mid init)$, and the conditional joint probability of Δa and ΔI given no subsequent reversal $P(\Delta I, \Delta a \mid no\ rev)$. From this, the we calculated conditional probability of a subsequent reversal (i.e., initiation) given input bias and model response, $P(init \mid \Delta I, \Delta a)$, for each time-point.

In the vicinity of the median state $(\Delta I_M, \Delta a_M)$, the log reversal probability varies almost linearly with ΔI and Δa (Fig. 4 b, quality of linear regression $r^2 > 0.99$). The three perceptual parameters - sensitivity, stability, and exploration - were defined to parametrize this dependence. Stability was defined as the gradient vector, or, equivalently, as the tangent of the slope, at the median state $tan(\beta) = \sqrt{\gamma_I^2 + \gamma_A^2}$. Stability was defined as the difference between the median and neutral levels of $\log P_{init}$, $-\gamma_I \Delta I_M - \gamma_A \Delta A_M$. Exploration was defined as the direction of the gradient vector at the median state $sin(\alpha) = \frac{\gamma_A}{\sqrt{\gamma_I^2+\gamma_A^2}}$. These definitions are presented alongside visualizations in Supplementary figure 2.

5 Data availability

The eye tracking datasets are available from the authors on request.

6 Computer code

The code used to extract reversal sequences is available via `https://github.com/cognitive-biology/Cumulative-smooth-pursuit-analysis-of-BR-OKN`.

The code used for computational modeling and simulated experiments is available from the authors on request.

References

[1] Sowell, E. R. et al. Mapping cortical change across the human life span. Nat. Neurosci. 6, 309–315 (2003).

[2] Paus, T. et al. Maturation of white matter in the human brain: A review of magnetic resonance studies. Brain Res. Bull. 54, 255–266 (2001).

[3] Geidd, J. N. Structural magnetic resonance imaging of the adult brain. Ann. N. Y. Acad. Sci. 1021, 77–85 (2004).

[4] Gomez-Robles, A., Hopkins, W. D., Schapiro, S. J. & Sherwood, C. C. Relaxed genetic control of cortical organization in human brains compared with chimpanzees. Proc. Natl. Acad. Sci. U. S. A. 112, 14799–14804 (2015).

[5] Foulkes, L. & Blakemore, S. J. Studying individual differences in human adolescent brain development. Nat. Neurosci. 21, 315–323 (2018).

[6] Stiles, J., Brown, T. T., Haist, F. & Jernigan, T. L. Brain and Cognitive Development. in Handbook of Child Psychology and Developmental Science 1–54 (John Wiley & Sons, Inc., 2015). doi:10.1002/9781118963418.childpsy202.

[7] Lebel, C., Treit, S. & Beaulieu, C. A review of diffusion MRI of typical white matter development from early childhood to young adulthood. NMR Biomed. 32, 1–23 (2019).

[8] Giedd, J. N., Raznahan, A., Mills, K. L. & Lenroot, R. K. Review: Magnetic resonance imaging of male/female differences in human adolescent brain anatomy. Biol. Sex Differ. 3, 1–9 (2012).

[9] Ruigrok, A. N. V. et al. A meta-analysis of sex differences in human brain structure. Neurosci. Biobehav. Rev. 39, 34–50 (2014).

[10] Xin, J., Zhang, Y., Tang, Y. & Yang, Y. Brain Differences Between Men and Women: Evidence From Deep Learning. Front. Neurosci. 13, (2019).

[11] Váša, F. et al. Conservative and disruptive modes of adolescent change in human brain functional connectivity. Proc. Natl. Acad. Sci. U. S. A. 117, 3248–3253 (2020).

[12] Khundrakpam, B. S., Lewis, J. D., Zhao, L., Chouinard-Decorte, F. & Evans, A. C. Brain connectivity in normally developing children and adolescents. Neuroimage 134, 192–203 (2016).

[13] Whitaker, K. J. et al. Adolescence is associated with genomically patterned consolidation of the hubs of the human brain connectome. Proc. Natl. Acad. Sci. U. S. A. 113, 9105–9110 (2016).

[14] Paus, T., Keshavan, M. & Giedd, J. N. Why do many psychiatric disorders emerge during adolescence? Nat. Rev. Neurosci. 9, 947–957 (2008).

[15] Hauser, T. U., Will, G. J., Dubois, M. & Dolan, R. J. Annual Research Review: Developmental computational psychiatry. J. Child Psychol. Psychiatry Allied Discip. 60, 412–426 (2019).

[16] Bellman, R. Dynamic Programming. (1957).

[17] Sutton, R. S. & Barto, A. G. Reinforcement Learning: An Introduction. (MIT Press, 2018).

[18] Yang, S. C. H., Wolpert, D. M. & Lengyel, M. Theoretical perspectives on active sensing. Current Opinion in Behavioral Sciences vol. 11 100–108 (2016).

[19] Noel, J.-P. et al. Supporting generalization in non-human primate behavior by tapping into structural knowledge: Examples from sensorimotor mappings, inference, and decision-making. Prog. Neurobiol. 101996 (2021) doi:10.1016/j.pneurobio.2021.101996.

[20] Cisek, P., Puskas, G. A. & El-Murr, S. Decisions in changing conditions: The urgency-gating model. J. Neurosci. 29, 11560–11571 (2009).

[21] Carland, M. A., Thura, D. & Cisek, P. The Urge to Decide and Act: Implications for Brain Function and Dysfunction. Neuroscientist vol. 25 491–511 (2019).

[22] Tajima, S., Drugowitsch, J., Patel, N. & Pouget, A. Optimal policy for multi-alternative decisions. Nat. Neurosci. 22, 1503–1511 (2019).

[23] Pastukhov, A. et al. Multi-stable perception balances stability and sensitivity. Front. Comput. Neurosci. 7, 1–18 (2013).

[24] Braun, J. & Mattia, M. Attractors and noise: Twin drivers of decisions and multistability. NeuroImage vol. 52 740–751 (2010).

[25] Cao, R., Pastukhov, A., Aleshin, S., Mattia, M. & Braun, J. Instability with a purpose: how the visual brain makes decisions in a volatile world. bioRxiv 2020.06.09.142497 (2020) doi:10.1101/2020.06.09.142497.

[26] Brascamp, J., Sterzer, P., Blake, R. & Knapen, T. Multistable Perception and the Role of the Frontoparietal Cortex in Perceptual Inference. Annu. Rev. Psychol. 69, 77–103 (2018).

[27] Ukai, K., Ando, H. & Kuze, J. Binocular rivalry alternation rate declines with age. Percept. Mot. Skills 97, 393–397 (2003).

[28] Kovács, I. & Eisenberg, M. Human Development of Binocular Rivalry. in Binocular Rivalry 101–116 (2004). doi:10.7551/mitpress/1605.003.0008.

[29] Hudak, M. et al. Increased readiness for adaptation and faster alternation rates under binocular rivalry in children. Front. Hum. Neurosci. 5, 1–7 (2011).

[30] Beers, A. M. Characterizing Binocular Rivalry Across the Lifespan. (2016).

[31] Pitchaimuthu, K. et al. Occipital GABA levels in older adults and their relationship to visual perceptual suppression. Sci. Rep. 7, 1–11 (2017).

[32] Abuleil, D., Mcculloch, D. L. & Thompson, B. Older adults exhibit greater visual cortex inhibition and reducedvisual cortex plasticity compared to younger adults. Front. Neurosci. 13, 1–7 (2019).

[33] Robertson, C. E., Kravitz, D. J., Freyberg, J., Baron-Cohen, S. & Baker, C. I. Slower Rate of Binocular Rivalry in Autism. J. Neurosci. 33, 16983–16991 (2013).

[34] Freyberg, J., Robertson, C. E. & Baron-Cohen, S. Reduced perceptual exclusivity during object and grating rivalry in autism. J. Vis. 15, 1–12 (2015).

[35] Robertson, C. E., Ratai, E. M. & Kanwisher, N. Reduced GABAergic Action in the Autistic Brain. Curr. Biol. 26, 80–85 (2016).

[36] Karaminis, T., Lunghi, C., Neil, L., Burr, D. & Pellicano, E. Binocular rivalry in children on the autism spectrum. Autism Res. 10, 1096–1106 (2017).

[37] Spiegel, A., Mentch, J., Haskins, A. J. & Robertson, C. E. Slower Binocular Rivalry in the Autistic Brain. Curr. Biol. 29, 2948-2953.e3 (2019).

[38] Miller, S. M. et al. Slow binocular rivalry in bipolar disorder. Psychol. Med. 33, 683–692 (2003).

[39] Antonio Aznar Casanova, J., Amador Campos, J. A., Moreno Sánchez, M. & Supèr, H. Onset time of binocular rivalry and duration of inter-dominance periods as psychophysical markers of ADHD. Perception 42, 16–27 (2013).

[40] Vierck, E. et al. Further evidence for slow binocular rivalry rate as a trait marker for bipolar disorder. Aust. N. Z. J. Psychiatry 47, 371–379 (2013).

[41] Jia, T. et al. Difference in the binocular rivalry rate between depressive episodes and remission. Physiol. Behav. 151, 272–278 (2015).

[42] Xiao, G. et al. Slow Binocular Rivalry as a Potential Endophenotype of Schizophrenia. Front. Neurosci. 12, 1–9 (2018).

[43] Ye, X., Zhu, R. L., Zhou, X. Q., He, S. & Wang, K. Slower and less variable binocular rivalry rates in patients with bipolar disorder, OCD, major depression, and schizophrenia. Front. Neurosci. 13, 1–11 (2019).

[44] Jia, T. et al. Difference in binocular rivalry rate between major depressive disorder and generalized anxiety disorder. Behav. Brain Res. 391, 112704 (2020).

[45] Tsuchiya, N., Wilke, M., Frässle, S. & Lamme, V. A. F. No-Report Paradigms: Extracting the True Neural Correlates of Consciousness. Trends Cogn. Sci. 19, 757–770 (2015).

[46] Naber, M., Frässle, S. & Einhäuser, W. Perceptual Rivalry: Reflexes Reveal the Gradual Nature of Visual Awareness. PLoS One 6, e20910 (2011).

[47] Frässle, S., Sommer, J., Jansen, A., Naber, M. & Einhäuser, W. Binocular rivalry: Frontal activity relates to introspection and action but not to perception. J. Neurosci. 34, 1738–1747 (2014).

[48] Aleshin, S., Ziman, G., Kovács, I. & Braun, J. Perceptual reversals in binocular rivalry: Improved detection from OKN. J. Vis. 19, 5–5 (2019).

[49] Laing, C. R. & Chow, C. C. A Spiking Model for Binocular Rivalry. J. Comput. Neurosci. 12, 1–18 (2002).

[50] American Psychological Association. Diagnostic and statistical manual of mental disorders. (2013).

[51] Grant, B. F. et al. Prevalence, correlates, disability, and comorbidity of DSM-IV borderline personality disorder: Results from the Wave 2 National Epidemiologic Survey on Alcohol and Related Conditions. J. Clin. Psychiatry 69, 533–545 (2008).

[52] Guilé, J. M., Boissel, L., Alaux-Cantin, S. & Garny de La Rivière, S. Borderline personality disorder in adolescents: prevalence, diagnosis, and treatment strategies. Adolesc. Health. Med. Ther. Volume 9, 199–210 (2018).

[53] Daros, A. R., Zakzanis, K. K. & Ruocco, A. C. Facial emotion recognition in borderline personality disorder. Psychol. Med. 43, 1953–1963 (2013).

[54] Daros, A. R., Uliaszek, A. A. & Ruocco, A. C. Perceptual biases in facial emotion recognition in borderline personality disorder. Personal. Disord. Theory, Res. Treat. 5, 79–87 (2014).

[55] Fujiwara, M. et al. Optokinetic nystagmus reflects perceptual directions in the onset binocular rivalry in Parkinson's disease. PLoS One 12, 1–22 (2017).

[56] Heidi, L. The Shifting Boundaries Of Adolescence. Nature 554, 429–431 (2018).

[57] Johnson, M. B. & Stevens, B. Pruning hypothesis comes of age. Nature 554, 438–439 (2018).

[58] Fung, M. H. et al. Pubertal Testosterone Tracks the Developmental Trajectory of Neural Oscillatory Activity Serving Visuospatial Processing. Cereb. Cortex 30, 5960–5971 (2020).

[59] Killanin, A. D. et al. Development and sex modulate visuospatial oscillatory dynamics in typically-developing children and adolescents. Neuroimage 221, 117192 (2020).

[60] Gurvich, C., Hoy, K., Thomas, N. & Kulkarni, J. Sex differences and the influence of sex hormones on cognition through adulthood and the aging process. Brain Sci. 8, (2018).

[61] Hamson, D. K., Roes, M. M. & Galea, L. A. M. Sex Hormones and Cognition: Neuroendocrine Influences on Memory and Learning. Compr. Physiol. 6, 1295–1337 (2016).

[62] Martos-Moreno, G. Á., Chowen, J. A. & Argente, J. Metabolic signals in human puberty: Effects of over and undernutrition. Mol. Cell. Endocrinol. 324, 70–81 (2010).

[63] Shaw, P. et al. Neurodevelopmental trajectories of the human cerebral cortex. J. Neurosci. 28, 3586–3594 (2008).

[64] Li, R. et al. Developmental maturation of the precuneus as a functional core of the default mode network. J. Cogn. Neurosci. 31, 1506–1519 (2019).

[65] Rannevik, G. et al. A longitudinal study of the perimenopausal transition: altered profiles of steroid and pituitary hormones, SHBG and bone mineral density. Maturitas 21, 103–113 (1995).

[66] Araujo, A. B. & Wittert, G. A. Endocrinology of the aging male. Best Pract. Res. Clin. Endocrinol. Metab. 25, 303–319 (2011).

[67] Craik, F. I. M. & Bialystok, E. Cognition through the lifespan: Mechanisms of change. Trends Cogn. Sci. 10, 131–138 (2006).

[68] Harris, I. D., Fronczak, C., Roth, L. & Meacham, R. B. Fertility and the aging male. Rev. Urol. 13, e184-90 (2011).

[69] Eliot, L. Neurosexism: the myth that men and women have different brains. Nature vol. 566 453–454 (2019).

[70] Simmons, D. R. et al. Vision in autism spectrum disorders. Vision Res. 49, 2705–2739 (2009).

[71] Eisenlohr-Moul, T. A., DeWall, C. N., Girdler, S. S. & Segerstrom, S. C. Ovarian hormones and borderline personality disorder features: Preliminary evidence for interactive effects of estradiol and progesterone. Biol. Psychol. 109, 37–52 (2015).

[72] Kreiser, N. L. & White, S. W. ASD in Females: Are We Overstating the Gender Difference in Diagnosis? Clin. Child Fam. Psychol. Rev. 17, 67–84 (2014).

[73] Baron-Cohen, S. et al. Why are Autism Spectrum conditions more prevalent in Males? PLoS Biol. 9, (2011).

[74] Alaerts, K., Swinnen, S. P. & Wenderoth, N. Sex differences in autism: A resting-state fMRI investigation of functional brain connectivity in males and females. Soc. Cogn. Affect. Neurosci. 11, 1002–1016 (2016).

[75] Ferri, S. L., Abel, T. & Brodkin, E. S. Sex Differences in Autism Spectrum Disorder: a Review. Curr. Psychiatry Rep. 20, (2018).

[76] Montague, P. R., Dolan, R. J., Friston, K. J. & Dayan, P. Computational psychiatry. Trends in Cognitive Sciences vol. 16 72–80 (2012).

[77] Giedd, J. N. The Digital Revolution and Adolescent Brain Evolution. J. Adolesc. Heal. 51, 101–105 (2012).

[78] Stevens, M. C. The contributions of resting state and task-based functional connectivity studies to our understanding of adolescent brain network maturation. Neurosci. Biobehav. Rev. 70, 13–32 (2016).

[79] Hull, J. V. et al. Resting-state functional connectivity in autism spectrum disorders: A review. Front. Psychiatry 7, (2017).

[80] Hong, S. J. et al. Atypical functional connectome hierarchy in autism. Nat. Commun. 10, 1–13 (2019).

[81] Wolf, R. C. et al. Aberrant connectivity of resting-state networks in borderline personality disorder. J. Psychiatry Neurosci. 36, 402–411 (2011).

[82] Xu, T. et al. Network analysis of functional brain connectivity in borderline personality disorder using resting-state fMRI. NeuroImage Clin. 11, 302–315 (2016).

[83] Brainard, D. H. The Psychophysics Toolbox. Spat. Vis. 10, 433–436 (1997).

[84] Pelli, D. G. The VideoToolbox software for visual psychophysics: Transforming numbers into movies. Spat. Vis. 10, 437–442 (1997).

[85] Kleiner, M. et al. What's new in psychtoolbox-3. Perception 36, 1–16 (2007).

[86] Bühlmann, P. & Yu, B. Analyzing bagging. Ann. Stat. 30, 927–961 (2002).

[87] Lehky, S. R. Binocular rivalry is not chaotic. Proc. R. Soc. B Biol. Sci. 259, 71–76 (1995).

[88] Mamassian, P. & Goutcher, R. Temporal dynamics in bistable perception. J. Vis. 5, 361–375 (2005).

[89] Vattikuti, S. et al. Canonical Cortical Circuit Model Explains Rivalry, Intermittent Rivalry, and Rivalry Memory. PLOS Comput. Biol. 12, e1004903 (2016).

[90] Cohen, B. P., Chow, C. C. & Vattikuti, S. Dynamical modeling of multiscale variability in neuronal competition. Commun. Biol. 2, 1–11 (2019).

[91] Moreno-Bote, R., Rinzel, J. & Rubin, N. Noise-induced alternations in an attractor network model of perceptual bistability. J. Neurophysiol. 98, 1125–1139 (2007).

[92] Shpiro, A., Curtu, R., Rinzel, J. & Rubin, N. Dynamical Characteristics Common to Neuronal Competition Models. J. Neurophysiol. 97, 462–473 (2007).

[93] Curtu, R., Shpiro, A., Rubin, N. & Rinzel, J. Mechanisms for frequency control in neuronal competition models. SIAM J. Appl. Dyn. Syst. 7, 609–649 (2008).

[94] Shpiro, A., Moreno-Bote, R., Rubin, N. & Rinzel, J. Balance between noise and adaptation in competition models of perceptual bistability. J. Comput. Neurosci. 27, 37–54 (2009).

7 Acknowledgements

We acknowledge support from NKFI (Nemzeti Kutatási, Fejlesztési és Innovációs Hivatal) 110466 and 134370 to IK, and from DFG (Deutsche Forschungsgemeinschaft) BR987/3 and BR987/4 to JB, as well as helpful discussions with Alexander Pastukhov. We thank Péter Soltész, Doctoral School of Psychology, Eötvös Loránd University, Budapest, Hungary for carrying out an extensive pilot study before the current project, and Kinga Farkas, MD, PhD, Department of Psychiatry and Psychotherapy, Semmelweis University, for recruiting and diagnosing patients. We are indebted for the work of Tímea Jáger, a graphic artist who helped us to generate the final versions of the figures.

8 Author contributions

GZ designed, developed and performed behavioral experiments; SA analyzed eye movements and conducted computational modeling; ZU recruited and diagnosed BPD patients, all authors discussed the results and contributed to the final manuscript.

9 Competing interest

The authors declare no competing interests.